

ORIGINAL ARTICLE

Construction and validation of an immunity-related prognostic signature for lung squamous cell carcinoma

Qing Yue¹, Wei Han², Ziling Liu^{1*}, Zain Abbas³, Akmal Zubair⁴, Saba Beigh⁵, Hayaa Mohammad Alhuthali⁶, Hind A. Alzahrani⁷, Rasha Mohammed Saleem⁸, Nahed S. Alharthi⁹

ABSTRACT

Background: The major aim of this research article is to construct an immune-related validation for signature in lung squamous cell carcinoma (LUSC) through analysis integrated bioinformatics analysis.

Methods: We constructed an optimized prognostic risk model consisting of five prognostic IR-lncRNAs (PIR-lncRNAs) (AC107884.1, LCMT1-AS1, AL163051.1, AC005730.3, and LINC02635). We then performed an examination for survival as well as an unconstrained prognostic examination on the portending risk model to assess and validate the prognostic value of the model. Furthermore, we examined differential immune cells examination of for infiltration between the patients in the model suffering from high and low risk.

Results: In this review article, we obtained 546 differentially expressed genes and 21 immune-related genes, identified 654 immune-related lncRNAs (IR-lncRNAs) by co-expression network analysis, and identified 18 PIR-lncRNAs through analysis of univariate Cox. Through analyzing immune escape and immunotherapy, we verified that the influence of immunotherapy in high-risk group patients may be lower.

Conclusion: Our findings elucidate the intrinsic molecular biological link between the pathogenic genes of LUSC and immune cells, which has important exploration and reference significance by using precise as well as potential therapy including immunotherapy of patients suffering from LUSC, especially for high-risk patients.

Keywords: Genes relevant with immunity, lncRNAs, lung squamous cell carcinoma, prognostic risk model, immune cell infiltration, immunotherapy.

Background

LUSC which is an abbreviation of lung squamous cell carcinoma (LUSC) is a unique neurotic sort of large cellular cancer in the lungs, representing about 25%-30% of the total (1,2). LUSC ranks first in both first in both the dreariness and mortality of cellular breakdown caused by cancer in the lungs, as well as its occurrence is higher in men than in men than in women (3) and lung squamous cell carcinoma (LUSC). The pathogenesis of LUSC is still unclear, but smoking is the most important risk factor for LUSC (4). Some patients with LUSC may have any of the prominent indications in the early stage, but as the disease progresses, corresponding respiratory symptoms or related symptoms after cancer metastasis may appear (5). LUSC is mainly cured or relieved of symptoms and prolongs life through surgery, radiotherapy, and chemotherapy (6) But overall, LUSC

has a poor prognosis. Therefore, it needs an hour to investigate novel divining genes to identify low- and high-risk LUSC patients.

Various previous reports mentioned that genes related to immunity also called Immunity-related guanosine triphosphatases (IRGs) regulation have a critical importance in the occurrence as well as in the development

Correspondence to: Ziling Liu

*Department of Oncology, The First Hospital of Jilin University, Jilin, China.

Email: ziling@jlu.edu.cn

Full list of author information is available at the end of the article.

Received: 20 January 2023 | **Accepted:** 12 May 2023



of LUSC, affecting the lifespan and prognosis of patients suffering from LUSC. Liang et al. (7) this study tried to figure the role of fscin actin-bundling protein 1 (FSCN1 identified a protein named FSCN1 abbreviated as fscin actin-bundling protein 1 as the hub immune gene of LUSC and its involvement in the microenvironment of the tumor, as well as found that FSCN1 was involved in the expansion, movement, anti-apoptosis, and attack of LUSC cells. Kim et al. (8) found that LUSC suppressor gene mutations can hinder different miniature natural variables of invulnerable immune cells and stromal cells, and the declaration of genes connected with interleukin creation as well as lymphocyte separation is essentially down-regulated, which is the cross-activity of microenvironment of LUSC and tumor suppressors' key genes controlling immune system.

In this review, we recognized unique immune-related lncRNAs (IR-lncRNAs), predicted furthermore, approved the endurance as well as risk visualization of LUSC patients through a foretelling model, showed the distinctions in immune cell penetration among high-as well as low patients of LUSC, finally noticed the distinctions in the impact of immunotherapy in patients within various abruptly selected risk groups. The purpose of this paper is to further elucidate the intrinsic molecular biological link between the pathogenic genes of LUSC and immune cells, which has important exploration and reference significance for the precise and potential immunotherapy of LUSC patients, especially for high-risk patients.

Materials and Methods

Obtaining LUSC gene expression data and patient's clinical information

TCGA stands for The Cancer Genome Atlas which is an information database (<http://tcga-data.nci.nih.gov>) based on a research project of cancer growth research settled together by the National Human Genome Institute as well as the National Cancer Institute, giving a huge, free reference data set for disease research (9), its prognosis remains unsatisfactory. This study aimed to develop novel prognostic genes related to glycolysis in PDAC and to apply these genes to new risk stratification. Methods: In this study, based on the Cancer Genome Atlas (TCGA10). We gathered information and details about the gene expression of LUSC as well as clinical data of several suffering LUSC from the TCGA data set. A sum of 551 patient' samples was gathered, having 502 LUSCs and 49 typical paracancerous tissues. Afterward, all data cleaning and transformations were performed using custom R language and Perl scripts.

Differential expression analysis of IRGs

We first obtained a list of IRGs from two databases, IMMPort (<https://www.immport.org/home>) (11) as well as InnateDB (12) the exact mechanisms involved in colorectal cancer (CRC). Then, the LUSC whole expressional transcriptome matrix and IRGs list were used as input files of R language software, and several various expression of genes was analyzed and normal paracancerous critical samples through the R packages

limma and pheatmap (13), their characteristics and biological function in glioblastoma (GBM14), and the differentially expressed genes (DEGs) were obtained, and then differentially expressed IRGs (DE-IRGs) were extracted. Finally, we visualized the results with heatmaps (15). p -value less than 0.05 is considered to have a significant difference.

Co-expression analysis of IR-lncRNAs

To start with, the expression of the transcriptome framework of all LUSC tests was genotyped to recognize which RNAs were mRNAs and which among them were lncRNAs. Next, the expression matrix of DE-IRGs was read, and calculated by Pearson correlation test, and examination of mRNA (IR-mRNAs) co-expression as well as lncRNAs was done to determine IR-lncRNAs (16), the expression levels and biological functions of lncRNAs in IH have not been well-studied. This study aimed to analyze the expression profile of lncRNAs and mRNAs in proliferating and involuting IHs. Methods: The expression profiles of lncRNAs and mRNAs in proliferating and involuting IHs were identified by microarray analysis. Subsequently, detailed bioinformatics analyses were performed. Finally, quantitative real-time polymerase chain reaction (qRT-PCR17) complex and precisely regulated process that is critical for mammalian development. There is currently no description of the role of the long noncoding RNAs (lncRNAs). Pearson correlation coefficients >0.4 as well as p -values <0.05 were thought about genuinely significant (18). Finally, the result was visualized with a correlation network.

Screening of prognostic IR-lncRNAs (PIR-lncRNAs)

We first extracted the endurance status and endurance season of each LUSC patient in the clinical information file and merged them with the expression matrix of IR-lncRNAs (19) respectively. Their common genes were then intersected and obtained for further analysis. Correlation of gene expression and methylation levels, gene set enrichment analysis (GSEA). Then, through the endurance of R packages as well as survminer, all IR-lncRNAs reported to subject to univariate Cox analysis, and their expression levels and the survival status and survival time of patients were calculated and compared circularly, and the PIR-lncRNAs were screened out (20), a comprehensive overview of genes and tumor-infiltrating immune cells (TICs21) but the potential of immunotherapy in GAC is worthy of consideration. The purpose of this study was to develop a reliable, personalized signature based on immune genes to predict the prognosis of GAC. Here, we identified two groups of patients with significantly different prognoses by performing unsupervised clustering analysis of The Cancer Genome Atlas (TCGA). Finally, we visualized all PIR-lncRNAs using a forest plot (22).

A prognostic risk model of LUSC

A prognostic risk model of LUSC was constructed based on PIR-lncRNAs. We duplicated the overall levels of expression of each PIR-lncRNAs in each example by the factors inducing risk and addition of them into acquiring

the risk score for each sample (23,24) clinical treatment, and Epstein-Barr virus (EBV). When the calculation of the risk score of each selected sample was contrasted with the median of the calculated risk score, the classical arrangement of the whole group of patients suffering from LUSC into high-risk as well as low-risk was performed (25), several biomedical computational algorithms were employed to identify eight hub prognostic MRGs that were significantly relevant to OSC survival. These eight genes have important clinical significance and prognostic value in OSC. Subsequently, a prognostic index was constructed. Drug sensitivity analysis was used to screen the key genes in eight MRGs. Immunohistochemistry (IHC26).

Survival examination of the LUSC prognostic risk model

To compare the differential factors in endurance among patients who fall into the high and low-risk groups in the LUSC risk prognostic model, we performed a survival analysis (27,28). We input the matrix information of risk score and risk grouping into R software and defined the survival function *survdiff* with survival time and survival status as dependent variables and risk grouping as independent variables through the R packages *survival* and *survminer* (29). Finally, the result was displayed with a survival curve (30).

Independent prognostic analysis of the LUSC prognostic risk model

To verify the probability factors of the LUSC prognostic risk model we constructed whether it is able to be used as a prognostic factor for the patients suffering from LUSC all alone for other clinical traits, and we performed an independent prognostic analysis (31). We used the survival R package, by arranging as well as merging the risk data (counting endurance time, endurance status, risk score and gathering, quality expression of genes framework) and certain other characteristics which are clinical for almost all patients suffering from all LUSC patients (including the patient's age, gender, tumor stage, and so on) for univariate and multivariate independent prognostic analyses (32,33). The visualization of the outcome was finalized using forest plots.

Differential analysis among patients regarding immune cell infiltration in low and high-risk groups

To evaluate the infiltration of immune cells in LUSC, we calculated the distribution ratio and differentiation among approximately 22 immune cells including in low- and high-risk groups using cell classification (34). First, we used a customized R script and configuration file, through the R packages *e1071*, *preprocess Core*, and *limma*, to convert the LUSC transcriptome expression matrix to data transformation as well as infiltration of immune cell analysis for obtaining the infiltration of cells which are responsible for immunity in each sample (35). Next, the *reshape2*, *ggpubr*, and R packages *limma* were cited, as well as the LUSC risk score file was read to perform differential analysis on the infiltration level among each sample of immune cells (36) a hypoxic microenvironment is commonly observed that drives tumor growth, progression, and heterogeneity. Hypoxia

and tumor-infiltrating immune cells might be closely related to the prognosis of osteosarcoma. In this study, we aimed to determine the biomarkers and therapeutic targets related to hypoxia and immunity through bioinformatics methods to improve the clinical prognosis of patients. We downloaded the gene expression data of osteosarcoma samples and normal samples in the UCSC Xena database and GTEx database, respectively, and downloaded the validation dataset (GSE21257). The final outcome was visualized with a histogram as well as a boxplot. p-value lesser than that of 0.05 was thought of as critical.

Immune escape and immunotherapy analysis of LUSC

To identify which subgroups of patients suffering from LUSC among the low- and high-risk groups were better off receiving immunotherapy, we performed an analysis of several samples in the prognostic risk model using immunotherapy as well as immune escape (37) including colorectal cancer (CRC). First, we obtained the TIDE score matrix of each LUSC sample through a tern named TIDE abbreviated as the Tumor Immune Dysfunction and Exclusion database which can be accessed at (<http://tide.dfci.harvard.edu>) (38). Then, sample scores from low- and high-risk groups in the score matrix were cyclically calculated by the R packages *limma* and *ggpubr*. Finally, the result was visualized through a violin plot.

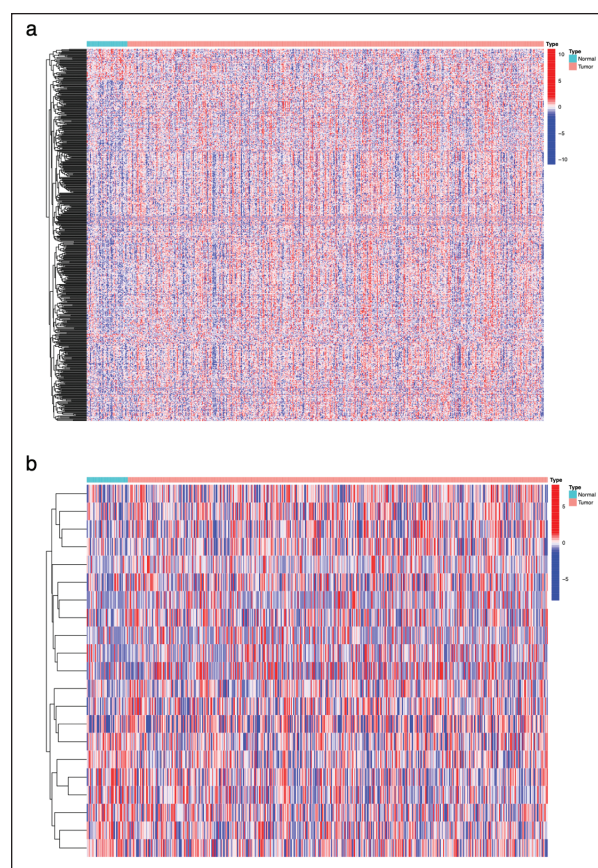


Figure 1. The heatmaps of the DEGs (a) and DE-IRGs (b). Red, up-regulated genes; blue, down-regulated genes. Cut-off criteria: $|FC| \geq 1.5$ and $p < 0.05$. By differential analysis of 60,660 transcript expression matrices from 502 LUSCs and 49 normal paracancerous samples, 546 DEGs and 21 DE-IRGs were found.

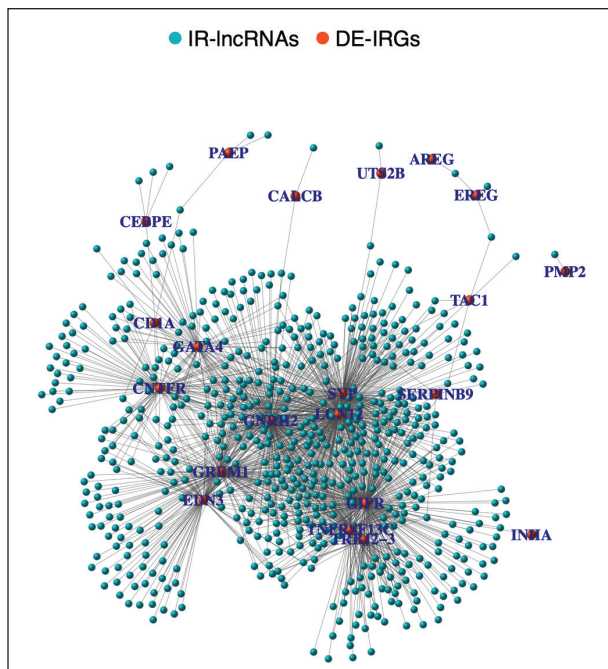


Figure 2. The co-articulation organization of DE-IRGs as well as IR-lncRNAs. Orange nodes address green nodes as well as DE-IRGs represent IR-lncRNAs. Dark grey strong lines address the coexpression connections among the DE-IRGs as well as IR-lncRNAs. Curated expression of 60,660 RNA transcript matrices using a database named TCGA database, including 16,901 lncRNAs and 19,962 mRNAs.

Results

Identification of DEGs and DE-IRGs in LUSC samples

By differential analysis of 60,660 transcript expression matrices from 502 LUSCs and 49 normal paracancerous samples, we obtained 546 DEGs, including 55 down-regulated DEGs and 491 up-regulated DEGs, as shown in Figure 1a. Meanwhile, we identified 21 DE-IRGs, including 7 down-regulated DE-IRGs and 14 up-regulated DE-IRGs, as shown in Figure 1b.

Identification of IR-lncRNAs in LUSC samples

We collected and curated 60,660 RNA transcript expression matrices using the database named as TCGA database, having 16,901 lncRNAs as well as mRNA 19,962. An expression matrix having 21 DE-IRGs was constructed based on the IMMPort and InnateDB databases. Co-expression network analysis identified 654 IR-lncRNAs. The relationship of the expression matrix, as well as the co-expression of IR-lncRNAs, was detailed and included in Valuable Records (IR-lncRNAs_Exp.xls as well as CoExp_network.xls). In addition, we built a co-expression and articulation of organization to imagine the relationship among DE-IRGs and IR-lncRNAs (Figure 2).

Identification of PIR-lncRNAs and development of prognostic risk model

Analysis through Univariate Cox was done on 654 IR-lncRNAs, and 18 PIR-lncRNAs were obtained, among which AP003071.2 and AC005730.3 were high-risk

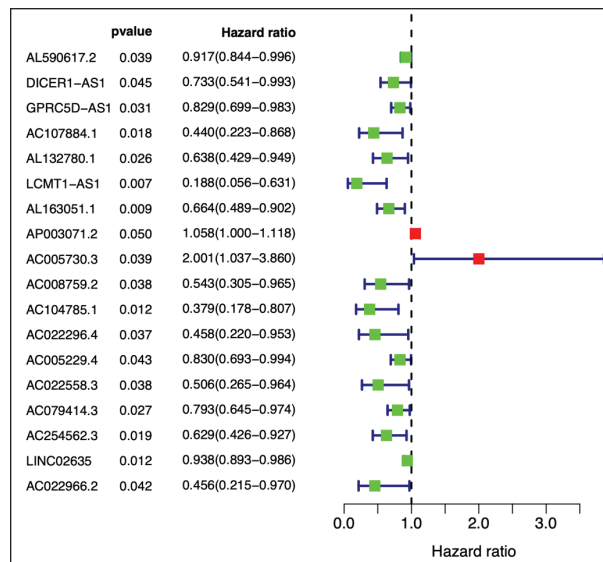


Figure 3. A univariate Cox regression examined the forest plot analysis of five PIR-lncRNAs of patients suffering from the LUSC. Red square, high HR value, green square, decreased HR value; and 95% confidence intervals of blue solid lines represent.

lncRNAs and the ratio calculated as [Hazard ratio (HR) >1], while AL590617.2, DICER1-AS1, GPC5D-AS1, AC107884.1, AL132780.1, LCMT1-AS1, AL163051.1, AC008759.2, AC104785.1, AC022296.4, AC005229.4, AC022558.3, AC079414.3, AC254562.3, LINC02635, and AC022966.2 were low-risk lncRNAs and the ratio calculated as (HR <1) (Figure 3). Using LASSO regression and cross-validation, an optimized prognostic risk model consisting of five PIR-lncRNAs (AC107884.1, LCMT1-AS1, AL163051.1, AC005730.3, and LINC02635) was finally obtained. The risk score file associated with the prognostic risk model was explained in the Supplementary novel data file (Risk.xls).

Evaluation and validation of the prognostic valuation of the model

After that, we performed an endurance and survival examination as well as a fully independent prognostic investigation on the prognostic risk model to assess and approve the prognostic worth of the model given for examination. The survival curve was portrayed by looking at the distinctions in endurance among patients in the low- as well as high-risk groups in the prognostic risk model. As displayed in Figure 4a, the survival of such patients surviving from LUSC in the high-risk group of LUSC was noticeably lower than the other examination low-risk group ($p < 0.05$). As can be seen from Figure 4b and c, in the calculated examination of univariate and multivariate the p-value of risk points was quite minimum than 0.05, as well as the HR value was higher than 1, recommending that the risk points in the prognostic risk model might be a solid clinically independent indicator which was quite important for reading.

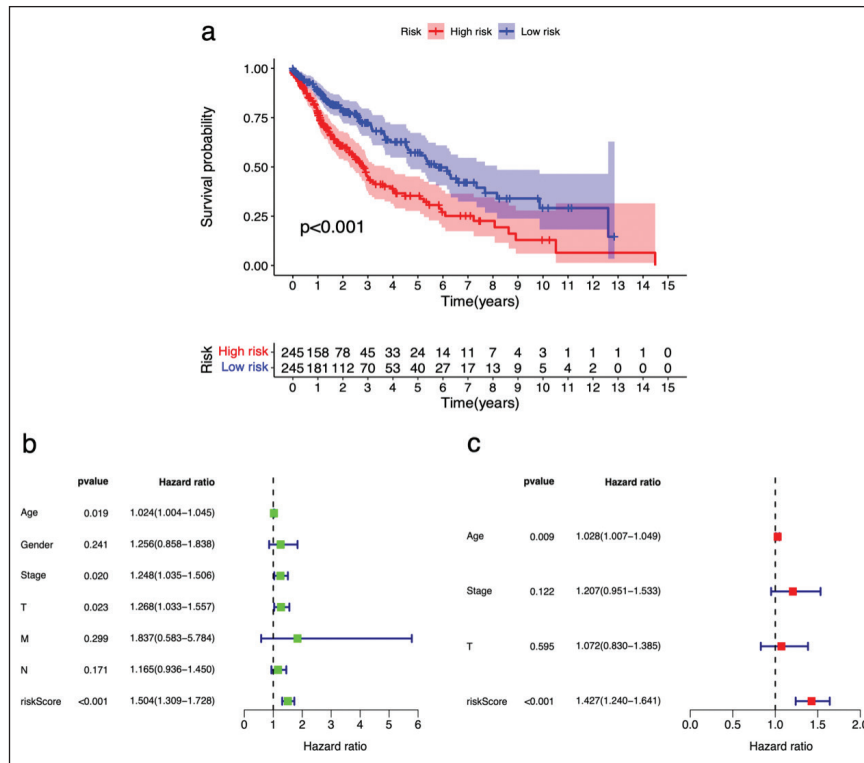


Figure 4. (a) The curve of survival in low-risk (blue) as well as high- (red) patients. Abscissa, the patient's survival years; the survival rate is ordinate. The mentioned lists underneath the bends showed the quantity of enduring patients each year. Univariate forest plots (b) as well as some of them are multivariate (c) strategic examination of clinical attributes in patients suffering from LUSC. Red or green square shows HR value, and the lines that are blue in color show approximately 95% confidence intervals.

Contrasts in infiltration in immune cells among patients of low and high risk

Differential analysis of infiltration in immune cells among patients having low and high risk in the prognostic risk model. Figure 5a summarizes the infiltration of different kinds of resistant cells in each example. As shown in Figure 5b, compared with the low-risk group, the other group classified as a high-risk group possessed a greater proportion of Natural Killer cells that were resting and activated Mast cells, whereas a lower number of naïve B-cells as well as resting Mast cells and Dendritic cells (p-value <0.05).

Contrasts in the efficacy of immune cells between low- and high-risk groups

Through the aforementioned analysis performed for immune escape as well as immunotherapy, we could see that patients present among the high-risk group have a greater TIDE score ($p < 0.001$), that is, greater the potential for immune escape, indicating in comparison with such patients that were placed at the low-risk group, the patients in the high-risk group receive Immunotherapy might be less effective (Figure 6).

Discussion

LUSC is included in most prominent respiratory malignancies. Despite systemic treatments such as surgery, radiotherapy, and chemotherapy, the general

visualization is as yet poor, particularly for patients with cutting-edge disease (39,40). Therefore, in this study, we obtained 546 DEGs and 21 DE-IRGs, identified 654 IR-lncRNAs by co-expression network analysis, and identified 18 PIR-lncRNAs by univariate by applying Cox analysis. Next, we designed an optimized model of prognostic risk consisting of five PIR-lncRNAs (AC107884.1, LCMT1-AS1, AL163051.1, AC005730.3, and LINC02635). After that, we examined survival and endurance examination as well as prognostic investigation independently on the prognostic risk model to survey and approve the prognostic worth of the model. After that, we examined differential analytical procedures for resistant immune cell penetration among models of low- and high-risk patients. At last, through the investigation of invulnerable immune cell escape and immunotherapy, we verified the performed immunotherapy in a group of patients may be lower in the high-risk group.

There is no published literature on the development of a risk prognostic model for patients suffering from LUSC in view of IR-lncRNAs. In any case, hardly any examinations have found that genes related to immunity as well as immune penetrating cells are assumed to have a significant role in the advancement of LUSC. Zhang et al. (41) figured out the prognostic clinical data of patients suffering from LUSC. Through deliberate systemic investigation of survival examination, they discovered that IRGs connected with prognosis as well as developed a prognostic risk model that possesses a

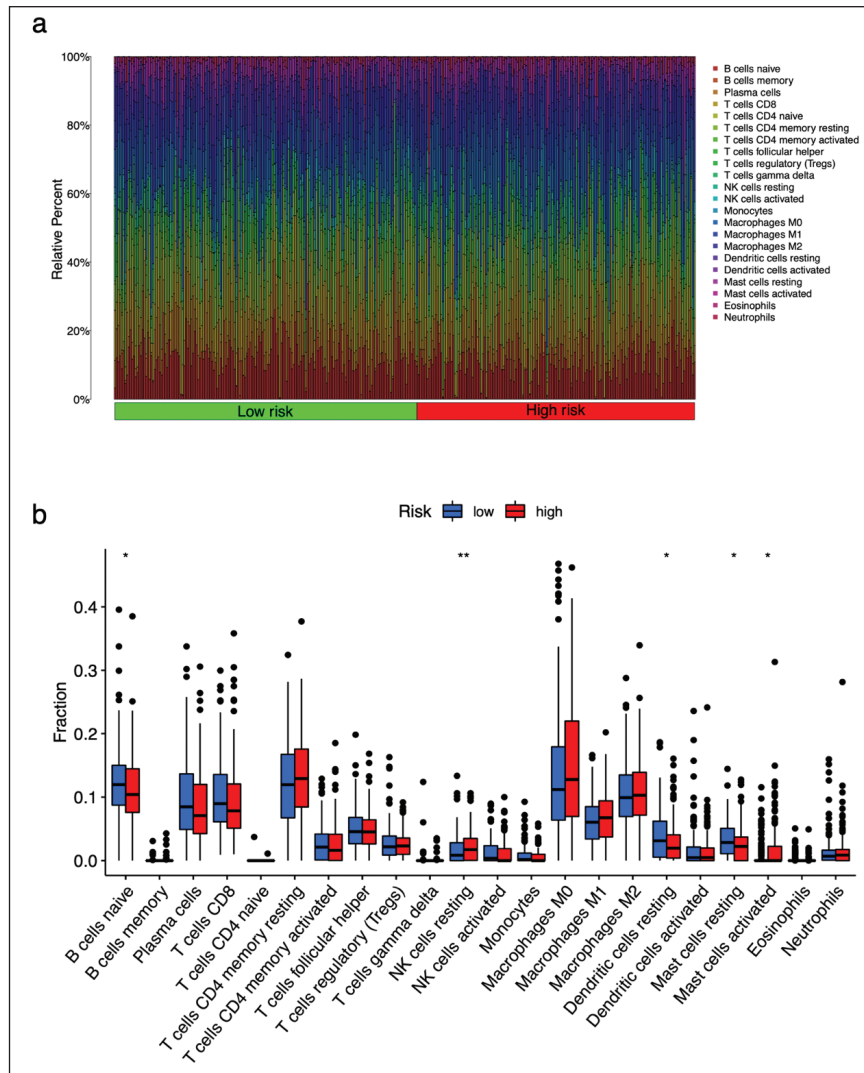


Figure 5. Contrasts of immune cell penetration among the low and high groups. (a) Abstract details of immune penetration in approximately 22 immune cell subpopulations from almost 551 numbers of samples. (b) Differential articulation-based violin plot of 22 invading immune cells. Abscissa: immune cell types, Red: high-risk bunch, Blue: generally known as a safe or low-risk group whereas ordinate: relative immune cell content.

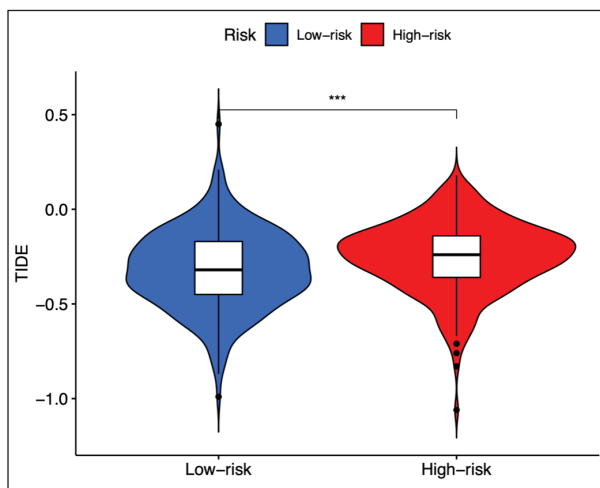


Figure 6. The violin plot of immune escape and immunotherapy analysis. Abscissa: Risk grouping, ordinate: TIDE score. Blue: low-risk group. ***, $p < 0.001$ as well as Red describes high-risk group.

calculated risk score that was emphatically related to five sorts of insusceptible immune cells (CD8 Lymphocytes, CD4 Immune system microorganisms, macrophages, neutrophils, and dendritic cells). Coincidentally, Zhuang et al. (42) characterized an insusceptible immune risk index denoted by Ischemia-reperfusion injury (IRI) by developing a prognostic model in view of 15 genes denoted as immune-related genes also known as r-IRGs and observed that IRI was a free prognostic variable (<0.001) and was firmly connected with the age of the patient (<0.05). In addition, dendritic cell and neutrophil penetration were essentially raised in the high IRI group (<0.05). Also, Rieke et al. (43) concentrated on the connection between methylation of genes responsible for DNA repair as well as CD274 (PD-L1) and CTLA4 articulation and discovered that the status of methylation as well as expression genes related to inflammation was firmly connected with LUSC and status of methylation of two genes was emphatically corresponded with expression of immune checkpoints.

Specific methylation of these genes can show a novel biomarker of inhibition in immune checkpoints.

In the current work, we examined differential analysis for the expression of DEGs and DE-IRGs, determined IR-lncRNAs via co-expression analysis of IR-mRNAs and lncRNAs, and screened out PIR-lncRNAs by univariate Cox analysis. After that, we developed a risk model for patients suffering from LUSC which was based on PIR-lncRNAs, and performed a comparative examination of survival as well as an independent prognostic examination of the LUSC risk model. Finally, differential analysis of immune escape as well as immune cells that were involved in infiltration among patients in low and high-risk groups was conducted.

Conclusion

Our findings will contribute to the discovery of novel IR-lncRNAs and immune cell infiltration signatures that affect LUSC's prognosis which then will be able to give valuable clinical help for potential immunotherapy of patients suffering from LUSC, specifically, those patients included in it which is suffering from high risk. Moreover, the current study shows certain limitations, like avoiding various clinical phenotypes of LUSC, as well as lacking in-depth research on the mechanism of signaling pathways. Talking about the future aspects following are the directions for further research plans and exploration.

Availability of data

The dataset that is utilized as well as during the examination performed in this might be conceded by reaching the corresponding author.

Conflicts of interest

The authors declare that they have no conflict of interest regarding the publication of this article.

Funding

This study got no subsidizing or any funding in any form.

Consent to participate

Not applicable.

Ethics approval

Not applicable.

Author details

Qing Yue¹, Wei Han², Ziling Liu¹, Zain Abbas³, Akmal Zubair⁴, Saba Beigh⁵, Hayaa Mohammad Alhuthali⁶, Hind A. Alzahrani⁷, Rasha Mohammed Saleem⁸, Nahed S. Alharthi⁹

1. Department of Oncology, The First Hospital of Jilin University, Jilin, China
2. Department of Hepatobiliary and Pancreatic Surgery, General Surgery Center, First Hospital of Jilin University, Jilin, China
3. Department of Life Sciences, University of Management and Technology, Lahore, Pakistan
4. Department of Biotechnology, Quaid-e-Azam University Islamabad, Islamabad, Pakistan
5. Department of Public Health, Faculty of Applied Medical Sciences, Albaha University, Albaha, Saudi Arabia
6. Department of Clinical Laboratory Sciences, College of Applied Medical Sciences, Taif University, Taif, Saudi Arabia

7. Basic Sciences, College of Applied Medical Sciences, Albaha University, Albaha, Saudi Arabia
8. Department of Laboratory Medicine, Faculty of Applied Medical Sciences, Albaha University, Albaha, Saudi Arabia
9. Department of Medical Laboratory Sciences, College of Applied Medical Sciences in Al-Kharj, Prince Sattam Bin Abdulaziz University, Al-Kharj, Saudia Arabia

Supplementary materials

The expression matrix as well as co-expression relationship belonging with IR-lncRNAs were detailed in Supplementary Files (IR-lncRNAs_Exp.xls and CoExp_network.xls). The risk score file associated with the prognostic risk model was explained inside the Supplementary File (Risk.xls). The corresponding author will provide the supplementary data upon request.

References

1. Zhang K, Han Z, Zhao H, Liu S, Zeng F. An integrated model of FTO and METTL3 expression that predicts prognosis in lung squamous cell carcinoma patients. *Ann Transl Med.* 2021 Oct;9(20):1523. <https://doi.org/10.21037/atm-21-4470>
2. Tan KT, Chen PW, Li S, Ke TM, Lin SH, Yang CC. Pterostilbene inhibits lung squamous cell carcinoma growth *in vitro* and *in vivo* by inducing S phase arrest and apoptosis. *Oncol Lett.* 2019 Aug;18(2):1631–40.
3. Xiong Y, Zhang X, Lin Z, Xiong A, Xie S, Liang J, et al. SFTA1P, LINC00968, GATA6-AS1, TBX5-AS1, and FEZF1-AS1 are crucial long non-coding RNAs associated with the prognosis of lung squamous cell carcinoma. *Oncol Lett.* 2019 Oct;18(4):3985–93. <https://doi.org/10.3892/ol.2019.10744>
4. Butler LM, Montague JA, Koh WP, Wang R, Yu MC, Yuan JM. Fried meat intake is a risk factor for lung adenocarcinoma in a prospective cohort of Chinese men and women in Singapore. *Carcinogenesis.* 2013 Aug;34(8):1794–9. <https://doi.org/10.1093/carcin/bgt113>
5. Sadeghi MM, Salama MF, Hannun YA. Protein kinase C as a therapeutic target in non-small cell lung cancer. *Int J Mol Sci.* 2021 May 24;22(11):5527. <https://doi.org/10.3390/ijms22115527>
6. Hamzawy MA, Abo-Youssef AM, Salem HF, Mohammed SA. Antitumor activity of intratracheal inhalation of temozolomide (TMZ) loaded into gold nanoparticles and/or liposomes against urethane-induced lung cancer in BALB/c mice. *Drug Deliv.* 2017 Nov;24(1):599–607. <https://doi.org/10.1080/10717544.2016.1247924>
7. Liang JS, Liu SQ, Yan CZ, Xiong M, Lin AY, Zhang X, et al. Role of FSCN1 in the tumor microenvironment of lung squamous cell carcinoma. *Immunobiology.* 2022 May;227(3):152206. <https://doi.org/10.1016/j.imbio.2022.152206>
8. Kim A, Lim SM, Kim JH, Seo JS. Integrative genomic and transcriptomic analyses of tumor suppressor genes and their role on tumor microenvironment and immunity in lung squamous cell carcinoma. *Front Immunol.* 2021 Feb 25;12:598671. <https://doi.org/10.3389/fimmu.2021.598671>
9. Song W, He X, Gong P, Yang Y, Huang S, Zeng Y, et al. Glycolysis-related gene expression profiling screen for prognostic risk signature of pancreatic ductal adenocarcinoma. *Front Genet.* 2021 Jun 23;12:639246. <https://doi.org/10.3389/fgene.2021.639246>

10. Wu R, Guo S, Lai S, Pan G, Zhang L, Liu H. A stable gene set for prediction of prognosis and efficacy of chemotherapy in gastric cancer. *BMC Cancer*. 2021 Jun 10;21(1):684. <https://doi.org/10.1186/s12885-021-08444-w>
11. Peng D, Gu B, Ruan L, Zhang X, Shu P. Integrated analysis identifies an immune-based prognostic signature for the mesenchymal identity in gastric cancer. *Biomed Res Int*. 2020 Apr 9;2020:9780981. <https://doi.org/10.1155/2020/9780981>
12. Shi JY, Bi YY, Yu BF, Wang QF, Teng D, Wu DN. Alternative splicing events in tumor immune infiltration in colorectal cancer. *Front Oncol*. 2021 Apr 29;11:583547. <https://doi.org/10.3389/fonc.2021.583547>
13. Wang J, Li Y, Xu B, Dong J, Zhao H, Zhao D, et al. *ALYREF* drives cancer cell proliferation through an *ALYREF-MYC* positive feedback loop in glioblastoma. *Oncol Targets Ther*. 2021 Jan 8;14:145–55. <https://doi.org/10.2147/OTT.S286408>
14. Pei J, Wang Y, Li Y. Identification of key genes controlling breast cancer stem cell characteristics via stemness indices analysis. *J Transl Med*. 2020 Feb 12;18(1):74. <https://doi.org/10.1186/s12967-020-02260-9>
15. Pan Y, Wu L, He S, Wu J, Wang T, Zang H. Identification of hub genes in thyroid carcinoma to predict prognosis by integrated bioinformatics analysis. *Bioengineered*. 2021 Dec;12(1):2928–40. <https://doi.org/10.1080/21655979.2021.1940615>
16. Yang K, Zhang X, Chen L, Chen S, Ji Y. Microarray expression profile of mRNAs and long noncoding RNAs and the potential role of PFK-1 in infantile hemangioma. *Cell Div*. 2021 Jan 11;16(1):1. <https://doi.org/10.1186/s13008-020-00069-y>
17. Ling YH, Zheng Q, Li YS, Sui MH, Wu H, Zhang YH, et al. Identification of lncRNAs by RNA sequencing analysis during *in vivo* pre-implantation developmental transformation in the goat. *Front Genet*. 2019 Oct 25;10:1040. <https://doi.org/10.3389/fgene.2019.01040>
18. Li Y, Xu J, Chen H, Bai J, Li S, Zhao Z, et al. Comprehensive analysis of the functional microRNA-mRNA regulatory network identifies miRNA signatures associated with glioma malignant progression. *Nucleic Acids Res*. 2013 Dec;41(22):e203. <https://doi.org/10.1093/nar/gkt1054>
19. Wang J, Zhao H, Dong H, Zhu L, Wang S, Wang P, et al. LAT, HOXD3 and NFE2L3 identified as novel DNA methylation-driven genes and prognostic markers in human clear cell renal cell carcinoma by integrative bioinformatics approaches. *J Cancer*. 2019 Oct 22;10(26):6726–37. <https://doi.org/10.7150/jca.35641>
20. Shi T, Gao G. Identify potential prognostic indicators and tumor-infiltrating immune cells in pancreatic adenocarcinoma. *Biosci Rep*. 2022 Feb 25;42(2):BSR20212523. <https://doi.org/10.1042/BSR20212523>
21. Mao R, Liu K, Zhao N, Guo P, Wu Y, Wang Z, et al. Clinical significance and prognostic role of an immune-related gene signature in gastric adenocarcinoma. *Aging (Albany NY)*. 2021 Jul 11;13(13):17734–67. <https://doi.org/10.18632/aging.203266>
22. Qian H, Li H, Xie J, Lu X, Li F, Wang W, et al. Immunity-related gene signature identifies subtypes benefitting from adjuvant chemotherapy or potentially responding to PD1/PD-L1 blockage in pancreatic cancer. *Front Cell Dev Biol*. 2021 Jun 23;9:682261. <https://doi.org/10.3389/fcell.2021.682261>
23. Yuan Y, Chen J, Wang J, Xu M, Zhang Y, Sun P, et al. Development and clinical validation of a novel 4-gene prognostic signature predicting survival in colorectal cancer. *Front Oncol*. 2020 May 20;10:595. <https://doi.org/10.3389/fonc.2020.00595>
24. Lai C, Zhang C, Lv H, Huang H, Ke X, Zhou C, et al. A novel prognostic model predicts overall survival in patients with nasopharyngeal carcinoma based on clinical features and blood biomarkers. *Cancer Med*. 2021 Jun;10(11):3511–23. <https://doi.org/10.1002/cam4.3839>
25. Zhang QF, Li YK, Chen CY, Zhang XD, Cao L, Quan FF, et al. Identification and validation of a prognostic index based on a metabolic-genomic landscape analysis of ovarian cancer. *Biosci Rep*. 2020 Sep 30;40(9):BSR20201937. <https://doi.org/10.1042/BSR20201937>
26. Chen C, Chen S, Cao H, Wang J, Wen T, Hu X, et al. Prognostic significance of autophagy-related genes within esophageal carcinoma. *BMC Cancer*. 2020 Aug 24;20(1):797. <https://doi.org/10.1186/s12885-020-07303-4>
27. Xu F, Xu H, Li Z, Huang Y, Huang X, Li Y, et al. Glycolysis-based genes are potential biomarkers in thyroid cancer. *Front Oncol*. 2021 Apr 26;11:534838. <https://doi.org/10.3389/fonc.2021.534838>
28. Guo P, Pu T, Chen S, Qiu Y, Zhong X, Zheng H, et al. Breast cancers with EGFR and HER2 co-amplification favor distant metastasis and poor clinical outcome. *Oncol Lett*. 2017 Dec;14(6):6562–70. <https://doi.org/10.3892/ol.2017.7051>
29. Klughammer J, Kiesel B, Roetzer T, Fortelny N, Nemc A, Nenning KH, et al. The DNA methylation landscape of glioblastoma disease progression shows extensive heterogeneity in time and space. *Nat Med*. 2018 Oct;24(10):1611–24. <https://doi.org/10.1038/s41591-018-0156-x>
30. Jin YW, Hu P. Tumor-infiltrating CD8 T cells predict clinical breast cancer outcomes in young women. *Cancers (Basel)*. 2020 Apr 26;12(5):1076. <https://doi.org/10.3390/cancers12051076>
31. Zhou C, Li C, Yan F, Zheng Y. Identification of an immune gene signature for predicting the prognosis of patients with uterine corpus endometrial carcinoma. *Cancer Cell Int*. 2020 Nov 9;20(1):541. <https://doi.org/10.1186/s12935-020-01560-w>
32. Wang M, Huang S, Chen Z, Han Z, Li K, Chen C, et al. Development and validation of an RNA binding protein-associated prognostic model for hepatocellular carcinoma. *BMC Cancer*. 2020 Nov 23;20(1):1136. <https://doi.org/10.1186/s12885-020-07625-3>
33. Feng Z, Qu J, Liu X, Liang J, Li Y, Jiang J, et al. Integrated bioinformatics analysis of differentially expressed genes and immune cell infiltration characteristics in esophageal squamous cell carcinoma. *Sci Rep*. 2021 Aug 17;11(1):16696. <https://doi.org/10.1038/s41598-021-96274-y>
34. Ren EH, Deng YJ, Yuan WH, Zhang GZ, Wu ZL, Li CY, et al. An immune-related long non-coding RNA signature to predict the prognosis of Ewing's sarcoma based on a machine learning iterative lasso regression. *Front Cell Dev Biol*. 2021 May 26;9:651593. <https://doi.org/10.3389/fcell.2021.651593>
35. Hu S, Liu H, Zhang J, Li S, Zhou H, Gao Y. Effects and prognostic values of miR-30c-5p target genes in gastric

- cancer via a comprehensive analysis using bioinformatics. *Sci Rep.* 2021 Oct 18;11(1):20584. <https://doi.org/10.1038/s41598-021-00043-w>
36. Liu D, Hu Z, Jiang J, Zhang J, Hu C, Huang J, et al. Five hypoxia and immunity related genes as potential biomarkers for the prognosis of osteosarcoma. *Sci Rep.* 2022 Jan 31;12(1):1617. <https://doi.org/10.1038/s41598-022-05103-3>
 37. Chen G, Wang L, Diao T, Chen Y, Cao C, Zhang X. Analysis of immune-related signatures of colorectal cancer identifying two different immune phenotypes: evidence for immune checkpoint inhibitor therapy. *Oncol Lett.* 2020 Jul;20(1):517–24. <https://doi.org/10.3892/ol.2020.11605>
 38. Zhang C, Zhang Z, Sun N, Zhang Z, Zhang G, Wang F, et al. Identification of a costimulatory molecule-based signature for predicting prognosis risk and immunotherapy response in patients with lung adenocarcinoma. *Oncoimmunology.* 2020 Sep 29;9(1):1824641. <https://doi.org/10.1080/2162402X.2020.1824641>
 39. Tang M, Li Y, Luo X, Xiao J, Wang J, Zeng X, et al. Identification of biomarkers related to CD8+ T cell infiltration with gene Co-expression network in lung squamous cell carcinoma. *Front Cell Dev Biol.* 2021 Mar 18;9:606106. <https://doi.org/10.3389/fcell.2021.606106>
 40. Makowiecki C, Nolte A, Sutaj B, Keller T, Avci-Adali M, Stoll H, et al. New basic approach to treat non-small cell lung cancer based on RNA-interference. *Thorac Cancer.* 2014 Mar;5(2):112–20. <https://doi.org/10.1111/1759-7714.12065>
 41. Zhang X, Xiao J, Fu X, Qin G, Yu M, Chen G, et al. Construction of a two-gene immunogenomic-related prognostic signature in lung squamous cell carcinoma. *Front Mol Biosci.* 2022 Apr 8;9:867494. <https://doi.org/10.3389/fmolb.2022.867494>
 42. Zhuang Y, Li S, Liu C, Li G. Identification of an individualized immune-related prognostic risk score in lung squamous cell cancer. *Front Oncol.* 2021 Mar 3;11:546455. <https://doi.org/10.3389/fonc.2021.546455>
 43. Rieke DT, Ochsenreither S, Klinghammer K, Seiwert TY, Klauschen F, Tinhofer I, et al Methylation of RAD51B, XRCC3 and other homologous recombination genes is associated with expression of immune checkpoints and an inflammatory signature in squamous cell carcinoma of the head and neck, lung and cervix. *Oncotarget.* 2016 Nov 15;7(46):75379–93. <https://doi.org/10.18632/oncotarget.12211>